Consiglio Nazionale delle Ricerche

PROGRAMMA
SHORT TERM MOBILITY
ANNO 2015

FINAL REPORT

TITOLO PROGRAMMA

ASSESSMENT OF RESIDUAL STRESS ON HEALED FRACTURE SURFACE OF THERMO REVERSIBLE MATRIX COMPOSITES

DIPARTIMENTO

SCIENZE CHIMICHE E TECNOLOGIE DEI MATERIALI

ISTITUZIONE OSPITANTE

KYOTO INSTITUTE OF TECHNOLOGY
CERAMIC PHYSICS LABORATORY
PROF. GIUSEPPE PEZZOTTI

PROT. AMMCNT-CNR 0002941 DEL 02/09/2015

PROPONENTE

DR. ALFONSO MARTONE

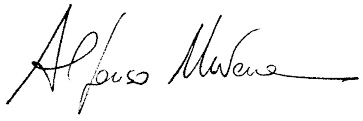

Assessment of Residual Stress On Healed Fracture Surface Of Thermo-Reversible Matrix Composites

Summary

The present document summarise the activities performed in the project carried out within the framework of the international cooperation agreement between *Consiglio Nazionale delle Ricerche* and JSPS "Short-time Mobility program".
Activities have been performed at Kyoto Institute of Technology, Ceramic Physics Lab on the supervision of Prof. Giuseppe Pezzotti.

1 Introduction

Composite materials are ideal candidates for structural applications due to high specific stiffness and strength and their excellent fatigue resistance. However, there are still concerns regarding their fracture toughness performance.
Common approach to reduce the susceptibility to such failure is the use of tridimensional reinforcement or the modification of the bulk resin by the addition of thermoplastic tougheners [1] or incorporating a microencapsulated healing agent that is released upon crack intrusion [2].
Integration of self-healing features within the hosting matrix would lead to a new vision in damage tolerance design management and also in the maintenance strategies of composite structures during operative life. Highly efficient recovery of structural integrity of the overall composite could be achieved by thermal treatment of the polymer matrix, according to service conditions experienced by the structure. Thermally reversible covalent bonding is a well establish approach to prepare self-healing polymers, as it does not rely on liquid resin delivery through microencapsulated systems, or embedded fibres. Therefore Diels–Alder (D-A) cycloaddition is a thermo-reversible reaction ideal for the synthesis of mendable polymers. Raman Piezospectroscopy has been successfully used for measure residual stress state for polymer composites [3-4]. Stress/strain field have been related to the Raman peaks shift or to the broadening of a band [4-5-6].
In this work, an epoxy system integrating thermos-reversible D-A adducts have been synthetized and characterized. The produced epoxy is able to recover damages, still preserving the pristine stiffness. The presented material is also suitable for the production of carbon fibre composite element. A methodology for measure stress field based on the RAMAN piezo-spectroscopy have been developed and implemented on composite samples.

2 Experimental

2.1 Materials

In this work, D-A adduct (2Ph2Epo) has been synthesised and added to DGEBA. The mixture has been subsequently cured using 4,4′-Diaminodiphenylmethane (DDM) and O,O′-Bis(2-aminopropyl) polypropylene glycol-block-polyethylene glycol-block-polypropylene glycol (Jeff 500) as curing agents.

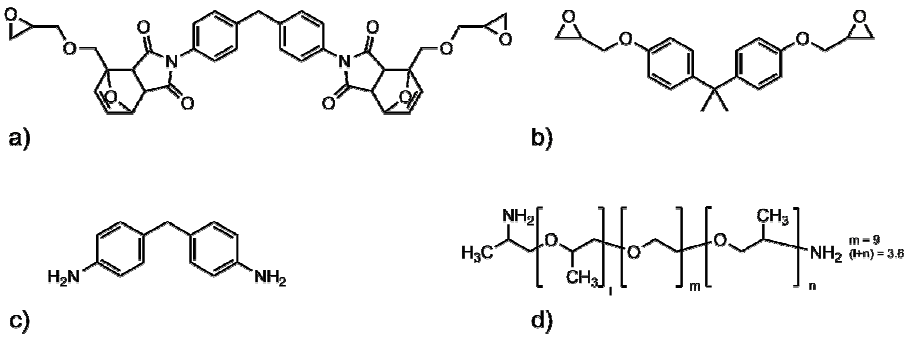

FIGURE 1. Resin components: a) 2Ph2Epo, b) DGEBA, c) DDM, d) Jeff 500

2.2 Methods

The T64000 Horiba/JobinYvon spectrophotometer equipped with blu LASER (514nm) was used. Spectra were collected from the surface of each specimen down to a maximum depth of 150 µm at step of 25 µm (position accuracy of 0.1 µm). The width of the examined spectral window depends on the excitation wavelength and especially on the acquisition mode of the spectrometer, double subtractive, or triple additive modes. Samples were mounted on a computer-controlled xyz stage, movable in 100 nm steps. The spectrometer was equipped with an Olympus microscope fitted with a 100X, 50X, 10X objectives.

Mechanical test were carried out on a universal testing machine equipped with 5kN load cell and fixture for three point bending loading.

3 Epoxy system able to recovery structural breakage

3.1 Evaluation of healing

During mechanical loading covalent bonds are exposed to intense stress, which eventually results in mechanical failure. Diels-Alder covalent bonds are weaker than other bonds in the polymer backbone, so that when loaded excessively they may break preferentially.

After breakage, a high temperature treatment is required in order to improve the healing efficiency. In fact, heating the sample above the rD-A threshold opens the Diels-Alder bonds resulting in high molecular mobility. This step is beneficial in promoting fracture rejoining and allowing molecular diffusion across the fracture rims. Thereafter, the last annealing at temperature corresponding to D-A reaction allows to regain the pristine mechanical properties due to restoration of network crosslinking density.

Diels Alder and retro Diels Alder equilibrium reactions have been studied by FTIR, monitoring the absorption band intensity related to vibrations of reversible linkage between 1,1'methylenedi-4,1-phenylene-bismaleimmide and glycidyl furfuryl ether. Unfortunately, the most significant diagnostic signals are weak in intensity. Therefore, the overall self-healing phenomenon and its thermomechanical effects has been studied on 2Ph2Epo65 crosslinked resin, and a more accurate characterization of D-A and rD-A reactions has been investigated further on the 2Ph2Epo pure epoxy adducts, taking advantage of the increased concentration of diagnostic bonds.

Figure 2 reports FTIR spectra of 2Ph2Epo65 crosslinked resin and of 2Ph2Epo neat adduct, in the healed or broken configuration as a consequence of different thermal treatments. As an invariant reference, the peak at 1700 cm^{-1} associated to C=O stretching of imide has been chosen.

Three signals have been selected to monitor the progress of D-A and rD-A reactions: the IR absorbance signals at 688 cm^{-1} associated to C-H bond attached to C=C and the peak at 832 cm^{-1} of C=C stretching vibration in the maleimide ring, and the signal at 1146 cm^{-1} associated to the asymmetric C–N–C stretch in 1,1'methylene di-4,1-phenylene-bismaleimmide and C–O–C stretch in furan ring.

The FTIR spectra were recorded on the cross-linked epoxy system after three different thermal treatments:

(a) after heating at 120°C and cooling to 90°C at 0.1 °C/min rate, (b) after heating at 120°C for 20 minutes and quenching to room temperature, (c) as prepared sample. While the 2Ph2Epo adduct has been analysed after heating at 120°C for 20 min and quenched to room temperature (a') and as prepared (b').

From comparison between spectra a' and b' it is clearly evident the presence of bands at 1146, 832 and 688 cm^{-1} in the "broken" configuration (a'), while the same absorption bands are not present in the spectrum b', related to the as prepared D-A adduct.

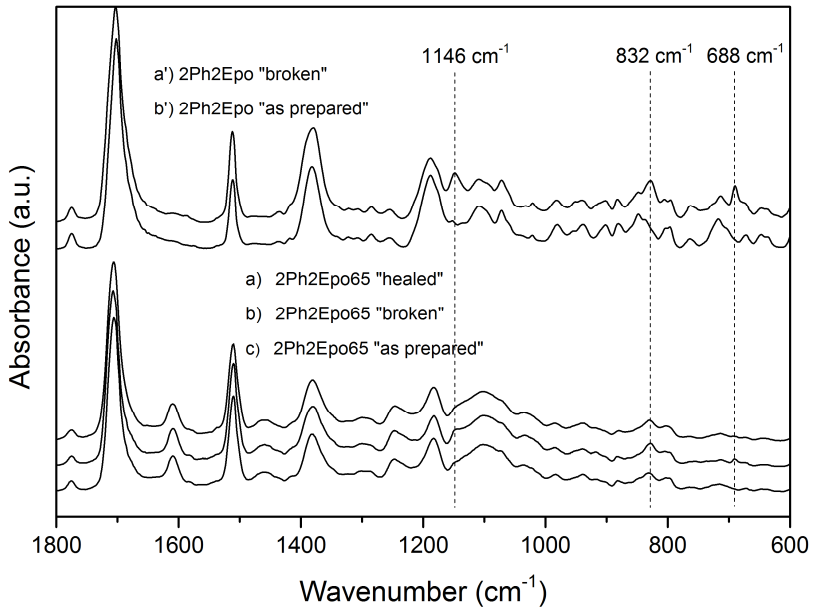

Figure 1- FTIR spectra: a) 2Ph2Epo65 "healed"; b) 2Ph2Epo65 "broken"; c) 2Ph2Epo65 "as prepared"; a') 2Ph2Epo "broken"; b') 2Ph2Epo "as prepared"

The same trend is evident for the crosslinked resin, although the selected peaks are much weaker. The most accurate information can be gained observing the trend of 688 cm^{-1} peak. It can be found in the b) sample, after thermal treatment at 120°C. Its absence can be verified in the pristine crosslinked resin (c), and it disappears again after healing cycle (a). A similar trend can be identified for the 1146 cm-1 band, although its observation is hindered by the presence of presence is other complex spectrum features. The band at 832 cm-1 cannot be used for the characterization of D-A reaction extent in the crosslinked sample.

After the treatment at 120°C, promoting the rD-A reaction, the intensities of these three absorption peaks increased due to D-A adduct rupture, as can be observed from figure 2. A further annealing at 90°C following the heat treatment at 120°C, strongly reduced the aforementioned peaks, resulting in a FTIR spectrum similar to the “as prepared” sample. This is a strong evidence that annealing at reduced temperature (90°C) promoted again the formation of D-A adduct, depleting the maleimide and furan groups during the D-A reaction.

The Raman spectra were recorded on 2Ph2Epo65 system after several thermal treatments: (a) as prepared sample; (b) after heating at 120°C for 20 minutes and quenching to room temperature (broken), (c) after heating at 120°C and cooling to 90°C at 0.1 °C/min rate (healed). The spectra (Figure 2a-c) evidence the intense absorption band at 1610 cm^{-1} attributed to the ring stretching. The absorbance of this sharp peak, identified as reference signal, remains constant with changes in D-A and rD-A reaction equilibrium. The signal at 1500 cm^{-1}, associated to C=C stretching vibration has been selected as detector of the progress of D-A and rD-A reactions.

In Figure 2a the spectrum was recorded on 2Ph2Epo65 as prepared; the occurrence of the rD-A reaction was observed in Figure 2b, after the thermal treatment at 120°C promoting the rD-A reaction: the increased peak at 1500 cm^{-1} was due to adducts breaking; the reversibility of the reaction was shown in figure 2c, following healing cycle treatment: the signal at 1500 cm^{-1} decreased again revealing the occurrence of the addition reaction between adduct precursors.

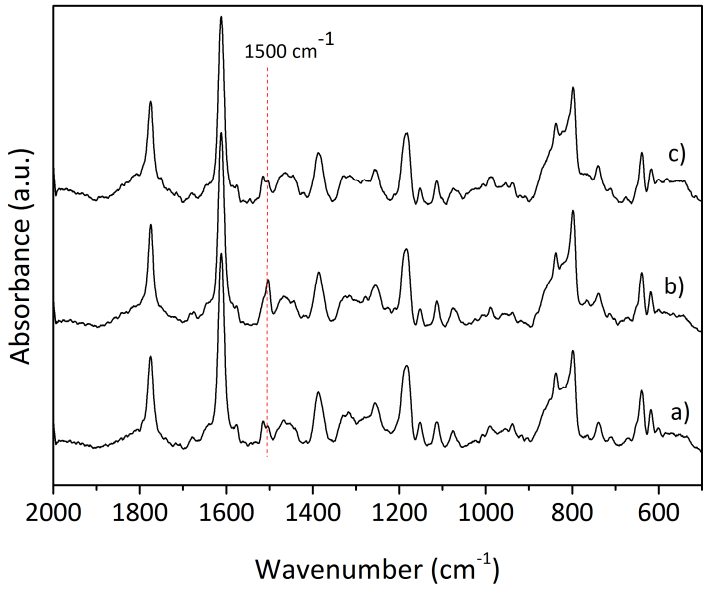

Figure 2- RAMAN spectra: a) 2Ph2Epo65 “as prepared”; b) 2Ph2Epo65 “broken”; c) 2Ph2Epo65 “healed”.

Quasi-static mechanical tests were carried out on specimens in order to evaluate the mechanical performances of the hybrid system. Figure 3 reports stress strain curve for 2Ph2Epo65 system. The broken samples were thermally treated at 90°C in order to restore mechanical properties and improve the healing fracture surface were brought closer together by polyamide adhesive film. Multiple healing was studied by repeating the test three times.

The virgin sample experienced elastic behaviour until 2% strain after that a plastic deformation occurred until the sample break at 3.5%. Healed sample exhibited the same stiffness (slope of the stress-strain curve) while them had a fragile fracture in the elastic region. The first healing led to a final strain of 1.8%, the second thermal treatment lead to 0.7 % strain at break. Since the sample were able to recover all their original stiffness, probably further thermal treatment could affect the DGEBA network, modifying the failure mechanism of the sample.

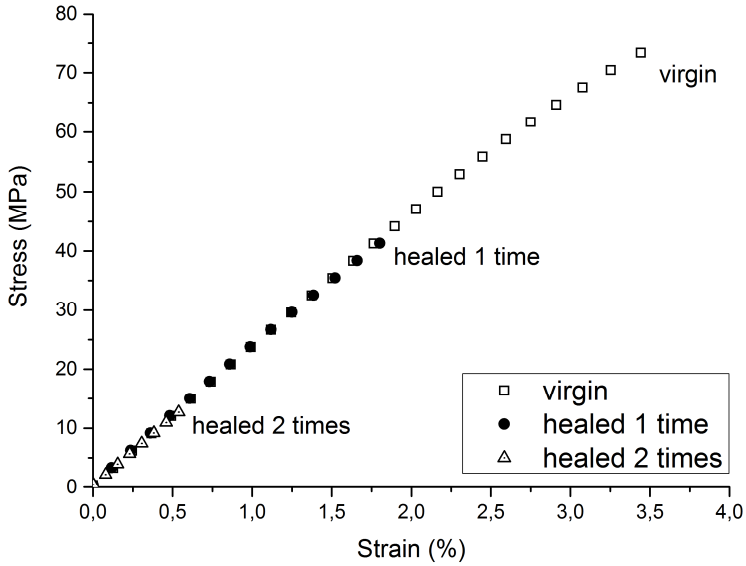

Figure 3 - Three point bending on virgin and healed system

The healing treatment allows a complete recover of mechanical stiffness (mean value 2.750 GPa) while the failure at break decreases.

3.2 Strain Sensor Identification

Micro-Raman spectroscopy should be used as non-destructive technique and provides information on the microscopic state of stresses in the constituents of materials with up to a micrometre of lateral and depth spatial resolutions [7-8].

The consistency of this technique relies on a linear correlation existing between Raman band broadening and stress reported for polymers such as polyethylene [5] [6]. Briefly, a probe volume is identified into the material through the focal point of a LASER beam. The observed intensity of Raman band is interpreted as an intensity distribution of scattered light around the focal point, described by the probe function. Raman band broadening is related to the frequency distribution of

the light scattered by each aromatic ring (1580-1620 cm^{-1}), thus depending on the deformation distribution of benzene groups inside the probe volume.

In our case, benzene ring stretch (1610 cm^{-1}) is clearly visible for the material at each status, as prepared – broken and healed. Thanks to the preponderance of benzene ring stretch intensity compared to other raman shift, the latter is considered as sensor for evaluating the deformation/stress status in the probe area.

a) b)

Figure 4 – Raman Investigation on deformed sample. a) the sample is deformed under 4 point bending mode b) the clamp is placed under laser ray for raman investigation

Figure 4 describe the clamp used for apply deformation to the sample. The load applied is recorded by load cell and the deflection by a mitutoyo micrometer head. Four point bending load is selected since the area between inner noses experiences pure bending load, indeed mapping the area across thickness in a section the stresses/strains pass from negative to positive linearly for small loads.

Figure 5 reports Raman spectra recorded along the thickness. Data were expressed through full width at half maximum (FWHM) of the Raman band located at 1610 cm^{-1} associated to the in-plane stretching vibration mode of the aromatic ring.

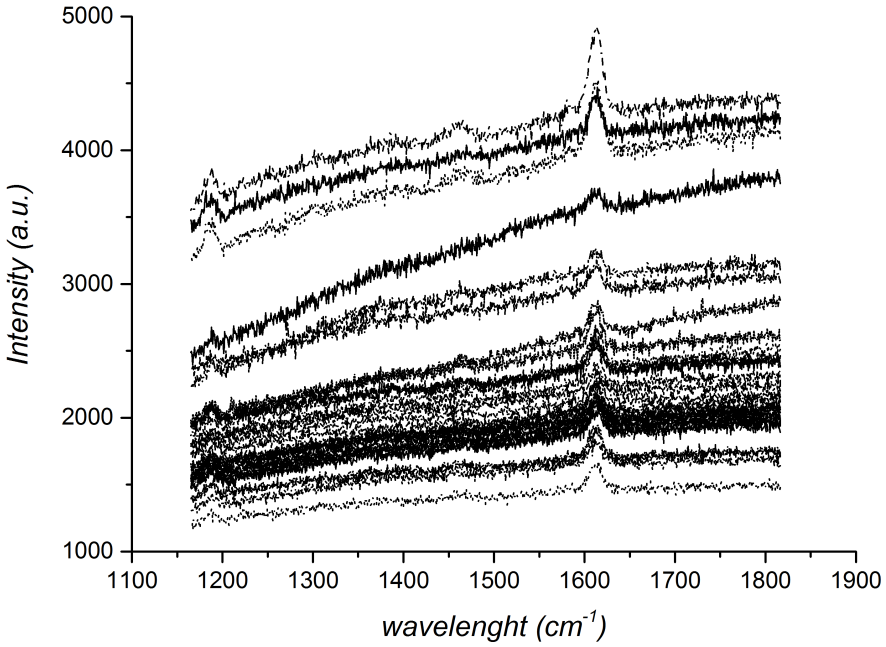

Figure 5 – Raman map along a section for the sample

The sample dimensions are 20x4x1 mm^3, during the test in order to achieve a maximum deformation on the sample to cover higher strain/stress conditions a span of 18 mm has been set up while the bending was applied on the 4 mm side. The sample was deformed under a load of 20 Newtons.

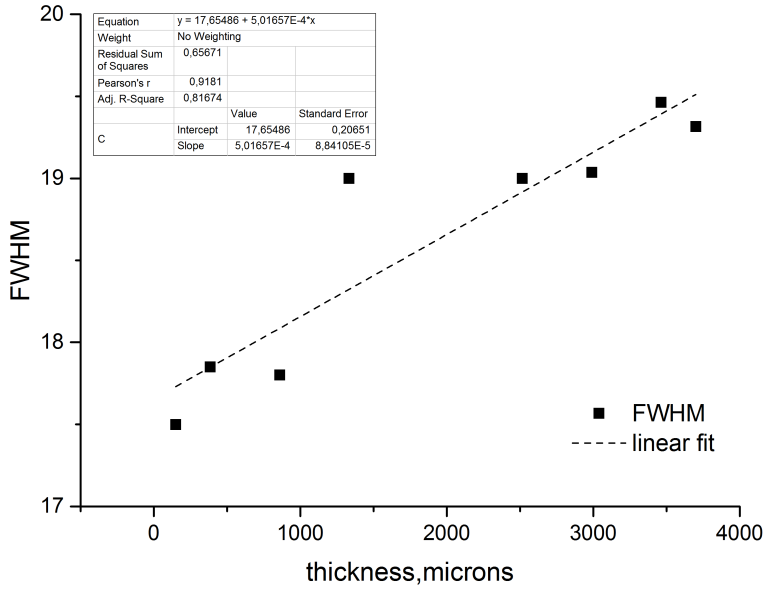

Figure 6 – Linear fit of data from raman map for the sample

Figure 6 reports the linear fitting of FWHM as evaluated by analysis of RAMAN spectra for each position. Further analysis based on the mechanics of 4 point bending beams should relate the strain achieved within the sample with the stress.

In the present case the 0 position is the negative stress point (compression) , while the 4000 microns position correspond to the positive stress region (tensile). Base on solid mechanics the stress along a section between noses is a linear function which is zero in the middle section and symmetrical.

The following expression allows the evaluation of maximum stress within the sample according to the ASTM Standard D6272 [9]

$$\sigma = \frac{3}{4}\frac{F\,L}{4\,w\,t} \qquad 1$$

Where σ is the tensile stress (MPa), F is the applied load, L the span, w is the sample width and t is the thickness.

The relation between full width at half maximum (FWHM, cm^{-1}) and stress experienced in the focal point is:

$$\sigma = \frac{FWHM - 18.62055}{0.048284} \qquad 2$$

4 Composites

4.1 Fabrication

Within this paragraph the main manufacturing stages for the preparation of a composite small plate will be discussed. Figure 7 shows the main stages during the manufacturing of such simple structures: a) dry unidirectional preform were cut and lied on a mould. A polyimide film is placed between in the middle plane in order to create a delamination; b) the dry fibres are impregnated with uncured 2Ph2Epo65; c) the material is crosslinked under vacuum bag for 24 hours at 90°C; d) hardened reversible fibre composite with the polyimide film creating an artificial delamination. A total of 12 unidirectional plies were laminated for a final thickness of 3 mm.

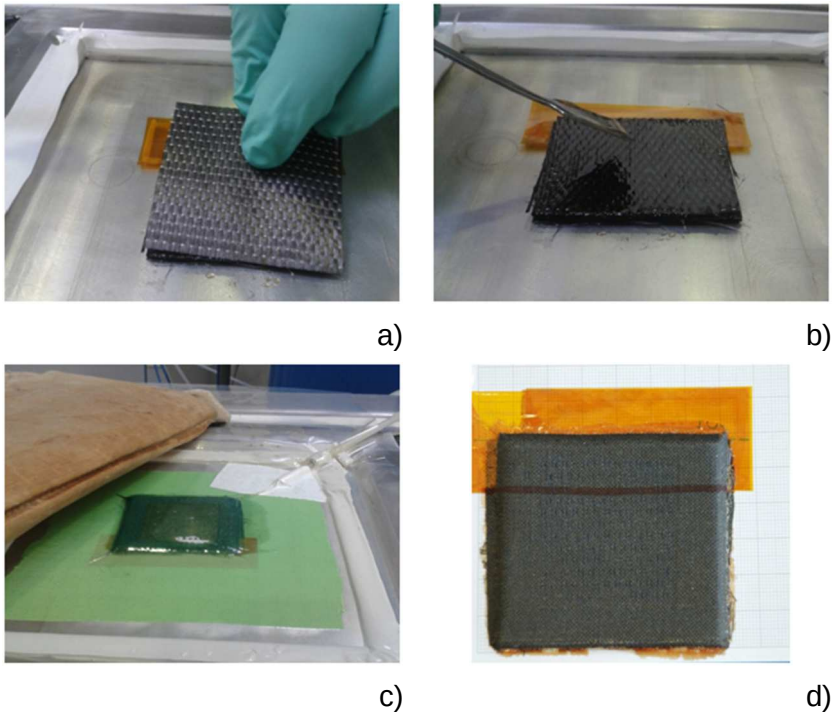

Figure 7 - . Manufacturing stages of the composite laminate: a) dry preforms with polyimide film in the mid-plane; b) reversible polymer addition; c) vacuum for composite consolidation; d) final coupon

Figure 8 reports two optical micrographs recorded on different sections to evaluate the coupons quality after the infusion process. Images show a uniform composite, without bubbles trapped among layers, with no fibre distortions.

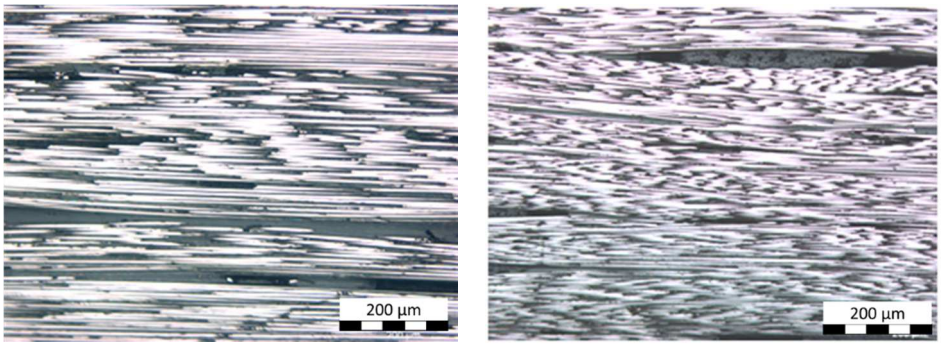

Figure 8 - Optical micrographs on a plate section containing fibres and reversible resin, 5X magnification.

4.2 Mechanical Tests

Interlaminar Shear Strength (ILSS) tests have been carried out according to ASTM D2344 [10]. For this, specimens sized 20x10x3 mm^3 cut from the infused and consolidated plate were prepared. In such test a high shear load is induced within the sample, leading to delamination or fibre failure (compression/traction) thereby offering relevant information about the amount of interlaminar strength recovered in the healed samples Figure 9 shows the test on a pristine sample (solid line) and on healed sample (dotted line). The mechanical evaluation was supported by optical analysis (micrographs) of the healed samples before and after the ILSS tests.

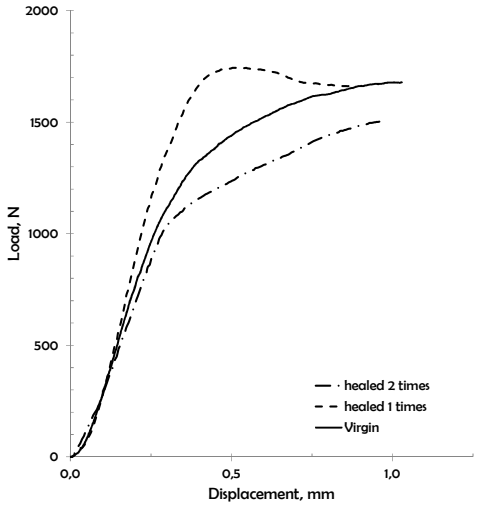

Figure 9 - Interlaminar shear strength curves

During the test the samples were completely deformed in the pin area (sample failure is inelastic, see Figure 10). Such plastic deformation can be presumably attributed to Diels-Alder bonds break-down.

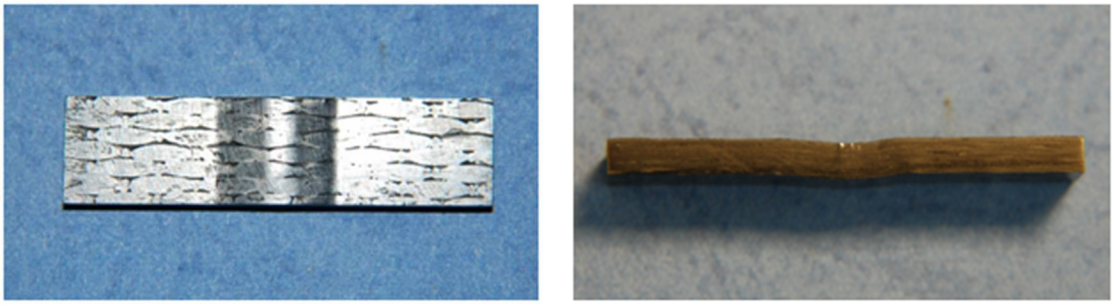

a) b)

Figure 10 - Sample deformation after the ILSS test. Failure mode is anelastic

Optical microscopy investigation revealed a failure due to fibre break in compression mode, and possible delaminations in the internal section of the specimen. The occurrence of fiber break affects the sample behaviour during tests subsequent to healing cycles. In fact, the fibres cannot undergo any healing, and discontinuity in reinforcement depress mechanical properties.

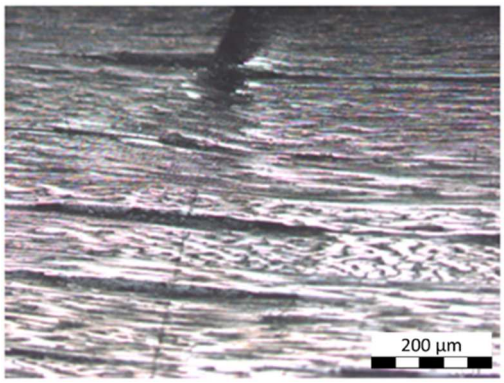

Figure 11 - ILSS sample micrograph (5X) after the test

After mechanical testing, the sample has been thermally treated for 20 min at 120°C and 24 hours at 90°C, according to the recovery treatment before a second ILSS test was repeated.
The sample recovered the initial geometry. The fracture is not evident anymore, having the epoxy matrix filled the gap rebonding fibre across the damaged portion. After healing, sample was re-tested resulting deformed as during the first test.
The load-displacement curve describing second test closely matches the behaviour observed for pristine sample (up to 700 N, 40% of maximum load). At higher deformations, the sample exhibits higher stiffness respect to the pristine status. Such behaviour could be attributed to small resin flow from the inner part of the composite sample, caused by mechanical compression during healing treatment. The limited resin depletion increases the fiber density in the composite, leading to higher stiffness. Moreover, the increased mobility of the epoxy molecules might also eliminate microdefects present in the structure.
ENF samples have an initial crack inserted within the material which promotes the crack propagation in mode II during the loading by sliding along middle plane. Figure 12a) reports the micrograph in the crack area, two polyimide films have been inserted on the middle plane, separating the upper and lower part of the sample. Samples with an initial crack allows the controlled failure avoiding the fibre breakage which could not be recovered by the system.
The ENF sample has been tested in three point bending configuration Figure 12b) reports the load displacement curve.

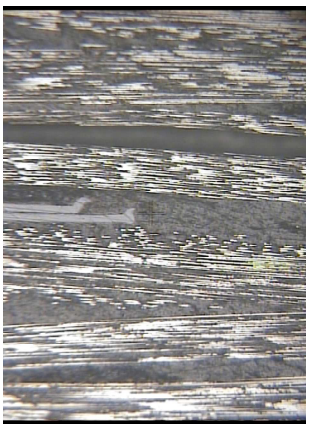

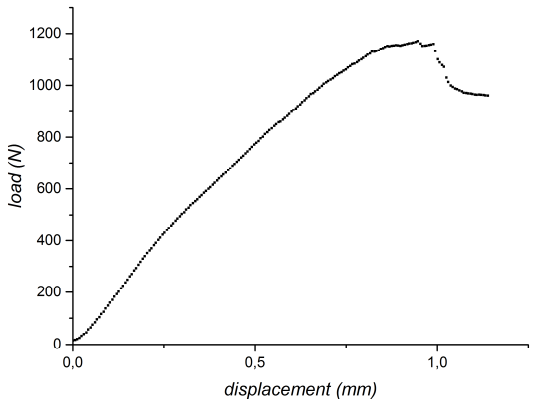

a) b)

Figure 12 – Optical micrograph (20X) of the ENF sample at crack tip a), load displacement curve during ENF test

4.3 Residual stresses

Raman maps were carried out on composites samples (ENF configuration) before and after the mechanical test in order to compare the modification of the stress field due to the failure occurred. Figure 13 reports the load configuration, the sample is bent with a constant load of 700 N.

Figure 13 – Composite sample under four point bending

The FWHM of the peaks recorded at 1610 cm^{-1} have been mapped by measuring raman spectra in the area of the crack tip. At the crack tip an area of 50x50 square microns have been mapped, results are reported in the picture below (Figure 14).

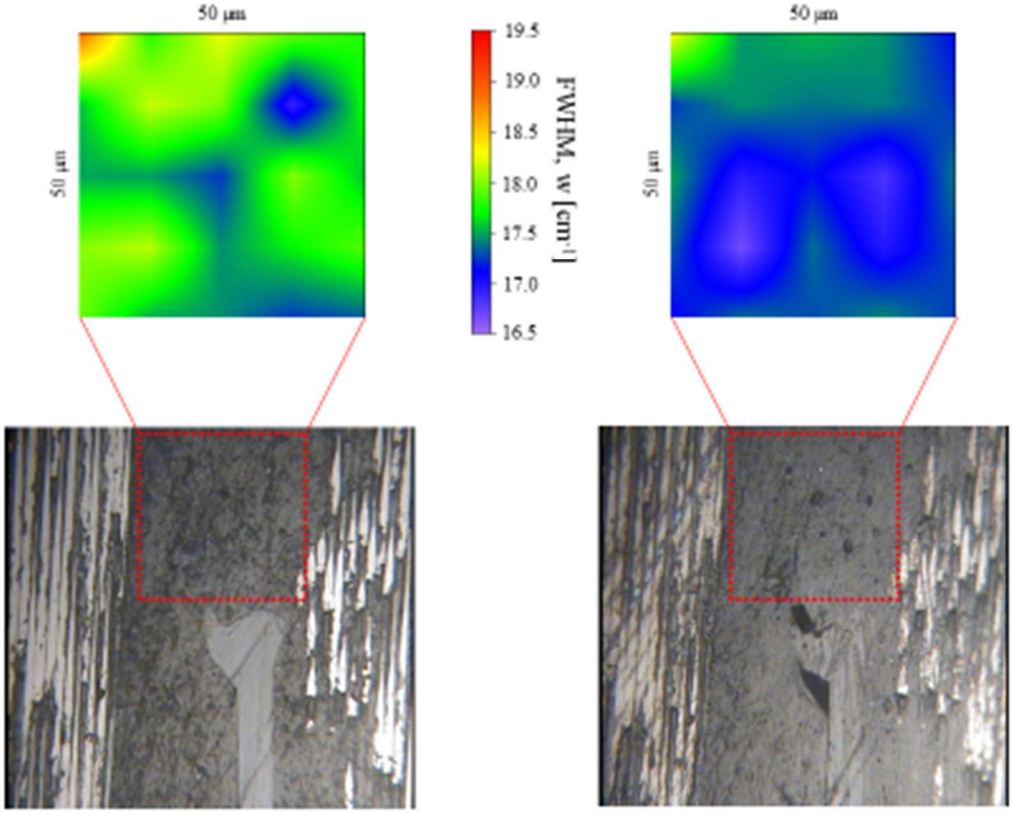

Figure 14 - Raman maps before and after the failure of the sample

Left side of the Figure 14 reports the contour plot for the healthy sample, lower picture reports the micrograph (50X) in the initial crack area, polyimide film is clearly visible. The investigated area is highlighted by a box, the upper picture describe the map of FWHM for the identified sensor.
Right side reports the analysis in the same area for the broken sample. On the micrograph it is possible to recognise the delamination, which correspond to the void at the crack tip.

By comparing the two contour plots the changes in stress field are detectable. Figure 15 reports the averaged FWHM for both areas. According to the calibration made on the pure epoxy for the sensor (equation 2) as effect of the failure a compressive stress state is induced at the crack tip.

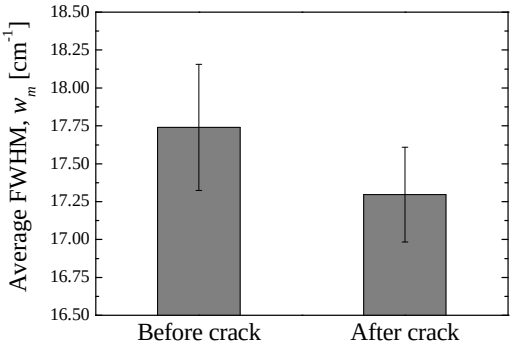

Figure 15 – Average FWHM at the crack tip.

5 Conclusions

In this work an epoxy system synthetized by integrating Diels-Alder epoxy adducts in a commercial epoxy system (DGEBA) has been studied and employed for manufacturing composite samples.
A methodology based on RAMAN piezo-spectroscopy has been set up on the system in order to measure the stress field upon a failure.
Further work will be focused on the study of the recovered area in order to evaluate residual stress in the healed region.

Acknowledgements

The author would like to thank Stefania Dello Iacono, Eugenio Amendola, Leonardo Puppulin Giuseppe Pezzotti for their support in experiments and data analysis.
I would also like to express my thanks to Antonella Poretti for her precious work at the CNR – International activities office.

References

[1] J. Hedrick, I. Yilger, G. Wilkes, J. McGrath, Chemical modification of matrix Resin networks with engineering thermoplastics, Polym. Bull. 13 (1985). doi:10.1007/BF00254652.

[2] S.R. White, N.R. Sottos, P.H. Geubelle, J.S. Moore, M.R. Kessler, S.R. Sriram, et al., Autonomic healing of polymer composites., Nature. 409 (2001) 794–7. doi:10.1038/35057232.

[3] C. Galiotis, A. Paipetis, C. Marston, Unification of Fibre/ Matrix Interfacial Measurements With Laser Raman Microscopy, J. Raman Spectrosc. 30 (1999) 899–912.

[4] B.P. Arjyal, D.G. Katerelos, C. Filiou, C. Galiotis, Measurement and modeling of stress concentration around a circular notch, Exp. Mech. 40 (2000) 248–255. doi:10.1007/BF02327496.

[5] M. Kyomoto, Y. Miwa, G. Pezzotti, Strain in UHMWPE for orthopaedic use studied by Raman microprobe spectroscopy, J. Biomater. Sci. Polym. Ed. 18 (2007) 165–178. doi:10.1163/156856207779116685.

[6] T. Kumakura, L. Puppulin, K. Yamamoto, Y. Takahashi, G. Pezzotti, In-depth oxidation and strain profiles in UHMWPE acetabular cups non-destructively studied by confocal Raman microprobe spectroscopy., J. Biomater. Sci. Polym. Ed. 20 (2009) 1809–22. doi:10.1163/156856208X386417.

[7] E. Anastassakis, A. Pinczuk, E. Burstein, F.H. Pollak, M. Cardona, Effect of static uniaxial stress on the Raman spectrum of silicon, Solid State Commun. 88 (1993) 1053–1058. doi:10.1016/0038-1098(93)90294-W.

[8] I. De Wolf, H.E. Maes, Mechanical stress measurements using micro-Raman spectroscopy, Microsyst. Technol. 5 (1998) 13–17. doi:10.1007/s005420050134.

[9] ASTM D6272 - 10 Standard Test Method for Flexural Properties of Unreinforced and Reinforced Plastics and Electrical Insulating Materials by Four-Point Bending, (n.d.). http://www.astm.org/Standards/D6272.htm (accessed February 9, 2016).

[10] ASTM D2344 / D2344M - 13 Standard Test Method for Short-Beam Strength of Polymer Matrix Composite Materials and Their Laminates, (n.d.). http://www.astm.org/Standards/D2344 (accessed February 9, 2016).